Supporting Information

Urine power cell with ammonium-intercalating electrodes: a novel approach to urine valorization coupled with CO_2 capture

Hanwoong Kim[a], Woohyuk Shin[a], Moon Son[b, c, *], Changsoo Lee[a, d, *]

[a] Department of Civil, Urban, Earth, and Environmental Engineering, Ulsan National Institute of Science and Technology (UNIST), 50 UNIST-gil, Eonyang-eup, Ulju-gun, Ulsan 44919, Republic of Korea

[b] Center for Water Cycle Research, Korea Institute of Science and Technology, 5 Hwarang-ro 14-gil, Seongbuk-gu, Seoul, 02792, Republic of Korea

[c] Division of Energy and Environment Technology, KIST-School, University of Science and Technology, Seoul, 02792, Republic of Korea

[d] Graduate School of Carbon Neutrality, Ulsan National Institute of Science and Technology (UNIST), 50 UNIST-gil, Eonyang-eup, Ulju-gun, Ulsan 44919, Republic of Korea

* Corresponding authors: M. Son (moonson@kist.re.kr); C. Lee (cslee@unist.ac.kr)

Number of pages: 13

Number of tables: 3

Number of figures: 9

Table S1 Composition of synthetic hydrolyzed urine.

	Typical concentration (g L^{-1})	Molar concentration (mM)
Formulation		
Na_2SO_4	2.3	8.1
NaH_2PO_4	2.1	17.5
NaCl	3.6	61.6
KCl	4.2	56.3
NH_4CH_3COO	9.6	124.6
NH_4HCO_3	21.4	270.9
NH_4OH (25%, w/w)	13 mL L^{-1} [a]	
Physicochemical properties		
Total ammonia nitrogen	7.8	559.9
Total inorganic carbon	3.3	270.9
Total organic carbon	1.5	124.6
Na^+	2.6	111.5
K^+	2.2	56.3
Cl^-	4.2	117.9
PO_4^{3-}	1.7	17.5
SO_4^{2-}	1.6	16.2

[a] NH_4OH was added by volume (mL L^{-1}).

Table S2 Physicochemical properties of hydrolyzed urine and of spent urine after CO_2 absorption.

Parameter	Unit	Hydrolyzed urine	Spent urine
pH		9.0 ± 0.0	7.6 ± 0.3
Conductivity	mS cm^{-1}	38.7 ± 0.7	51.9 ± 0.5
Total ammonia nitrogen	g L^{-1}	8.0 ± 0.0	7.9 ± 0.0
Total inorganic carbon	g L^{-1}	2.5 ± 0.0	4.4 ± 0.1
Na^+	g L^{-1}	2.5 ± 0.0	2.6 ± 0.0
K^+	g L^{-1}	2.4 ± 0.0	2.4 ± 0.0
Cl^-	g L^{-1}	4.4 ± 0.0	4.2 ± 0.1
PO_4^{3-}	g L^{-1}	1.6 ± 0.1	1.4 ± 0.1
SO_4^{2-}	g L^{-1}	1.7 ± 0.0	1.4 ± 0.0

Table S3 Performance of urine-ammonium power cells operated with diluted spent urine (SU) as high-salinity stream and freshwater (1 g L^{-1} NaCl) as low-salinity stream. Each condition was tested for at least three full cycles for each condition.

Dilution factor	Average PD (W m^{-2})	Cycle time (s)	Consumed SU (mL) [a]	Energy recovery (J)	Specific energy recovery (kJ m^{-3}) [b]
Undiluted	0.27 ± 0.02	2002 ± 74	500 ± 18	0.38 ± 0.03	0.8 ± 0.1
2-fold	0.23 ± 0.01	1687 ± 44	211 ± 5	0.27 ± 0.02	1.3 ± 0.1
10-fold	0.11 ± 0.01	1407 ± 54	35 ± 1	0.11 ± 0.01	3.1 ± 0.2

PD, power density.

[a] Expressed as the equivalent volume of undiluted SU consumed.

[b] Calculated per unit volume of equivalent undiluted SU consumed.

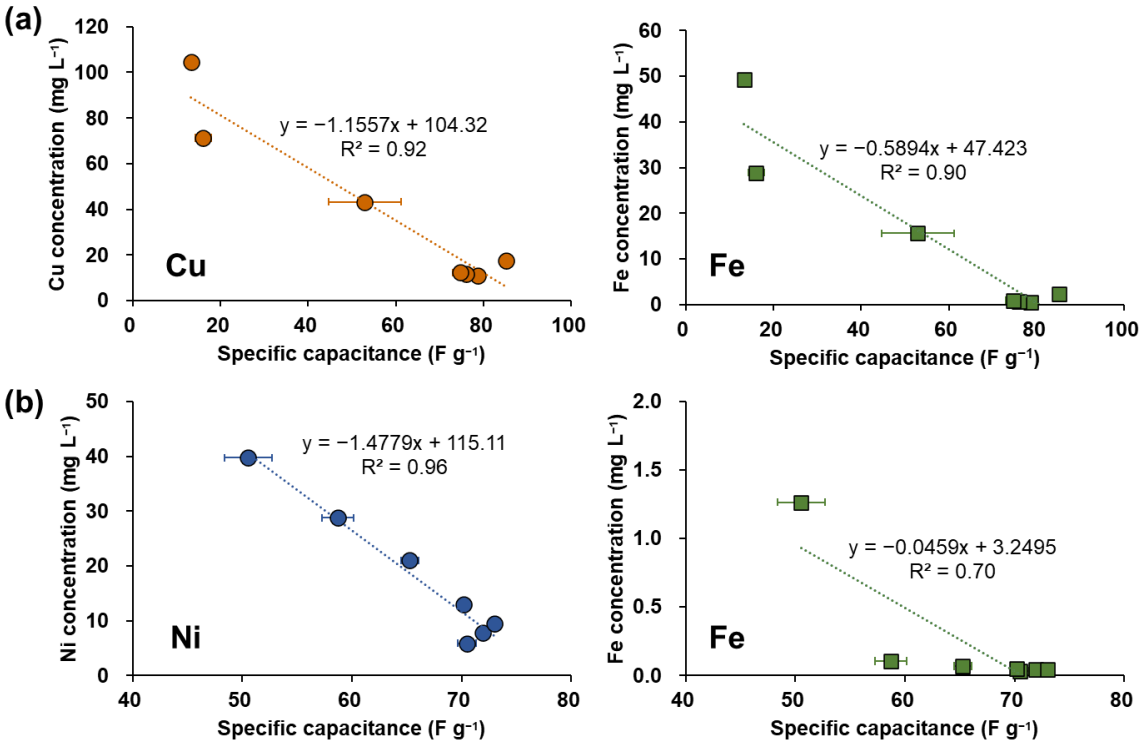

Fig. S1 Correlation between leached metal concentrations and specific capacitance from stability tests of (a) CuHCF and (b) NiHCF electrodes in 560 mM NH_4Cl solution across a pH range of 6.7 to 9.7. Initial measurements at pH 4.9 were excluded to avoid interference from residual surface metals originating from electrode synthesis.

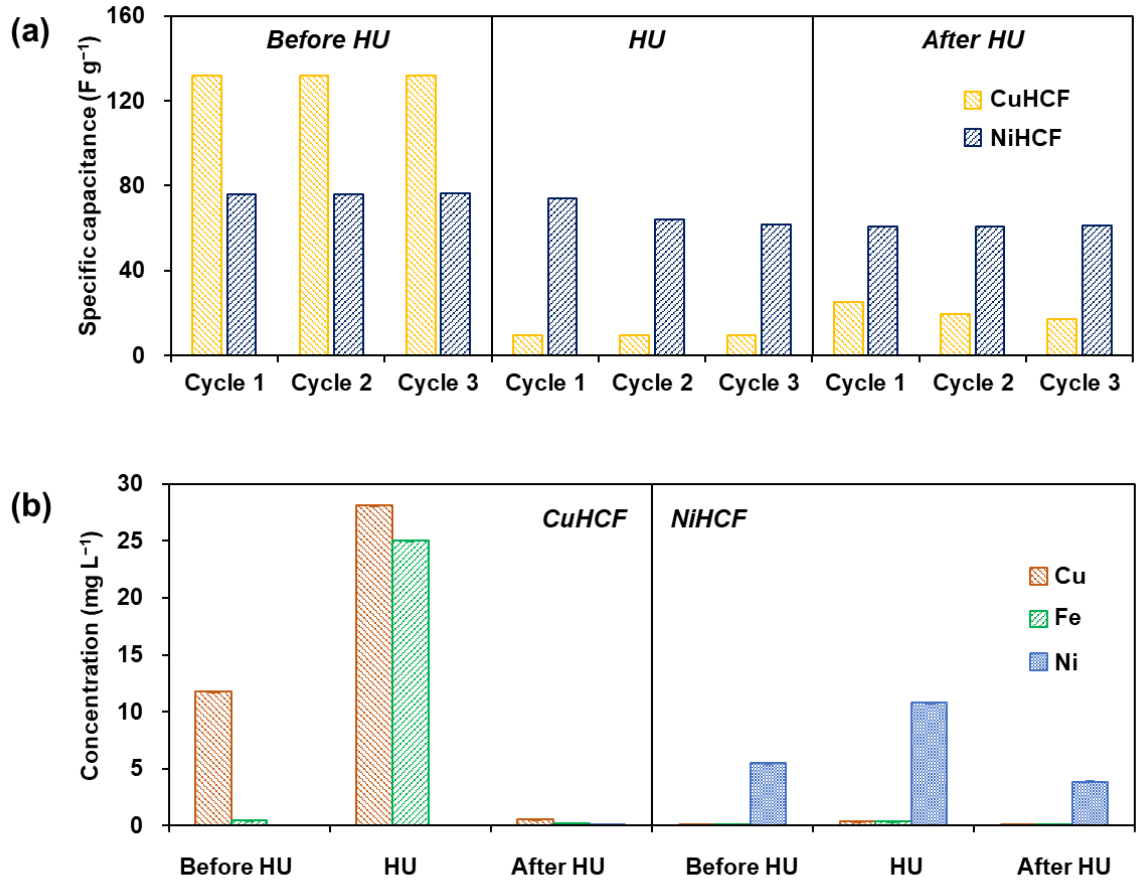

Fig. S2 Functional and structural degradation of CuHCF and NiHCF electrodes during stability tests in hydrolyzed urine (HU), conducted using cyclic voltammetry (CV): (a) specific capacitance values and (b) leached metal concentrations measured in each CV cycle. Additional CV measurements were carried out in 560 mM NH_4Cl solution (pH 4.9) both before and after HU exposure to assess baseline and post-exposure behavior. Three CV cycles were recorded for each condition.

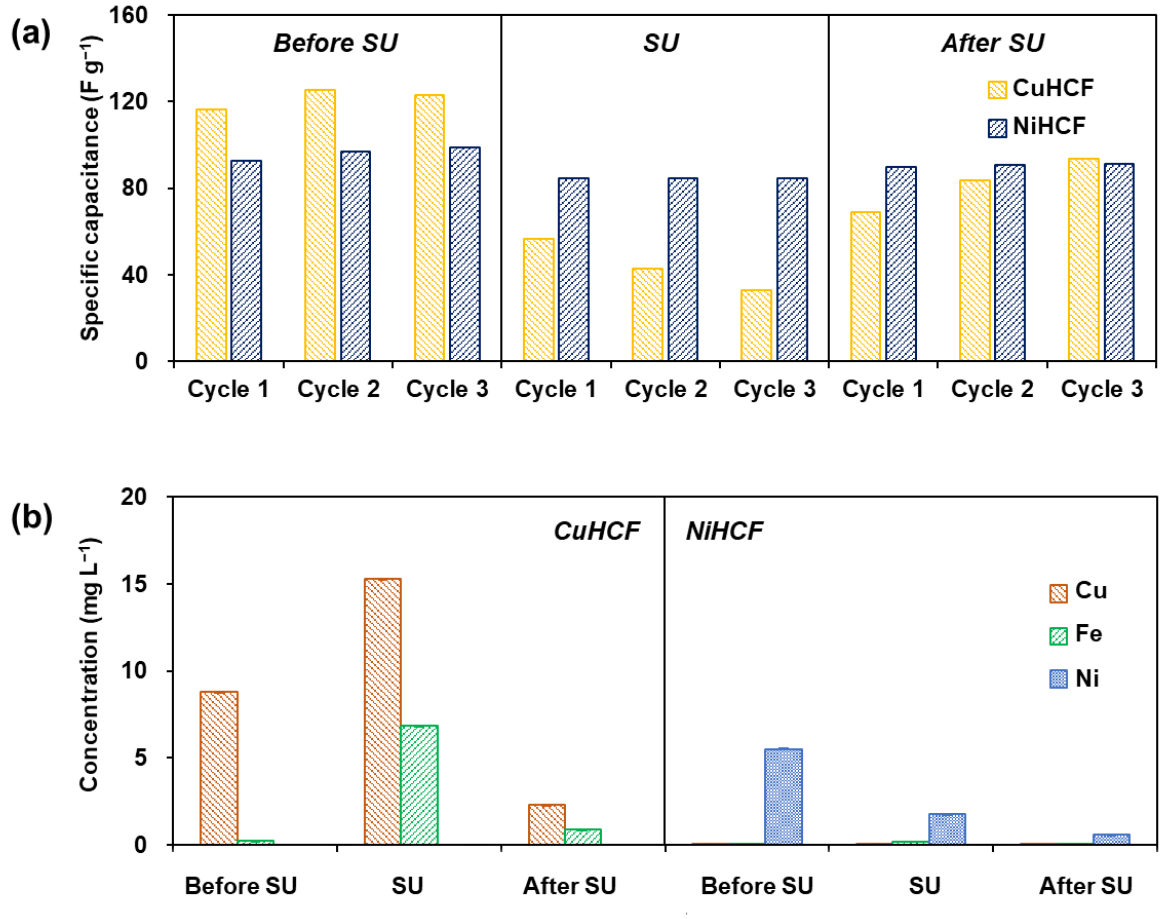

Fig. S3 Functional and structural degradation of CuHCF and NiHCF electrodes during stability tests in spent urine (SU), conducted using cyclic voltammetry (CV): (a) specific capacitance values and (b) leached metal concentrations measured in each CV cycle. Additional CV measurements were carried out in 560 mM NH_4Cl solution (pH 4.9) both before and after SU exposure to assess baseline and post-exposure behavior. Three CV cycles were recorded for each condition.

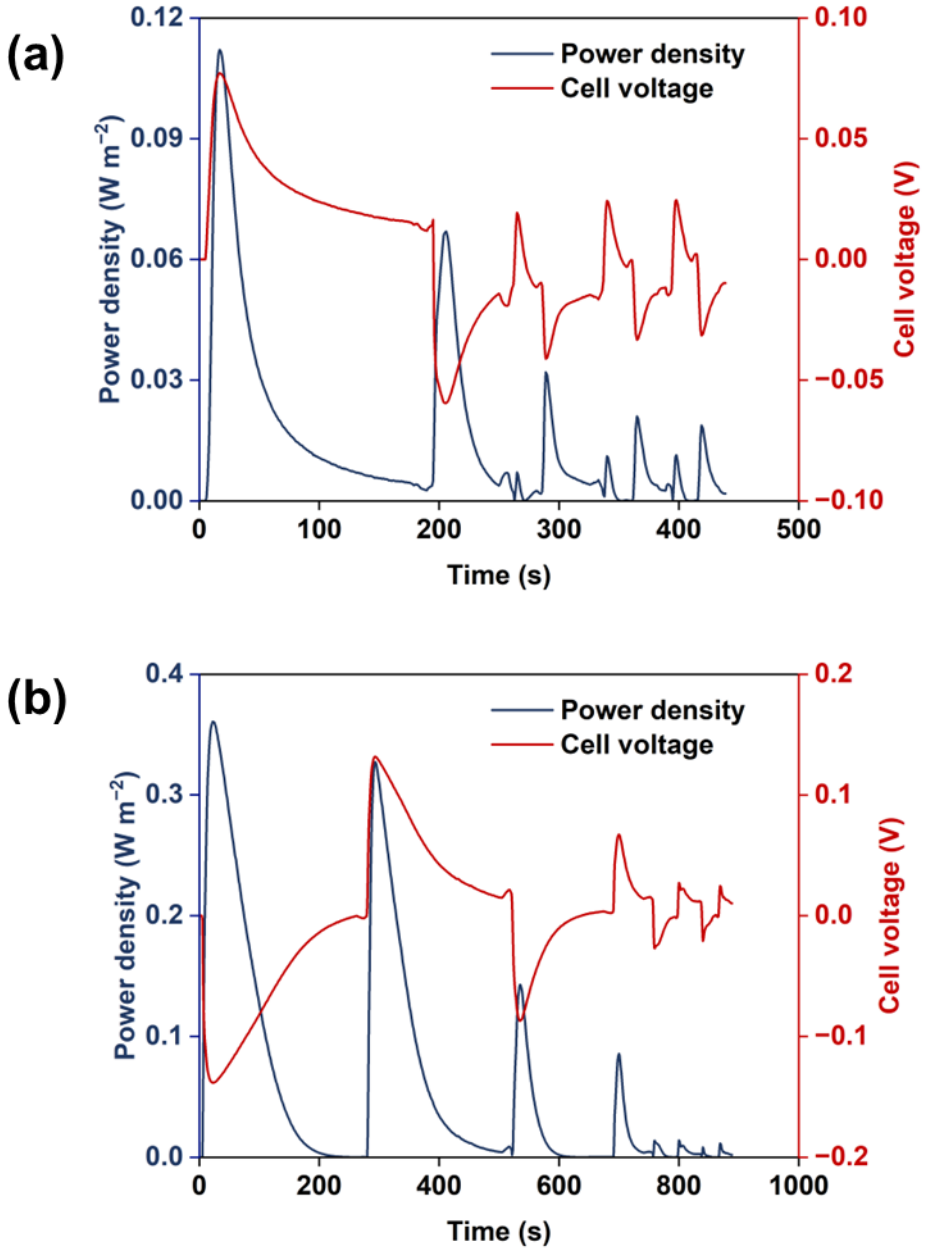

Fig. S4 Power density and cell voltage profiles of urine-ammonium power cell equipped with CuHCF electrodes, operated at an external resistance of 75 Ω using (a) hydrolyzed urine and (b) spent urine as low-salinity streams, with freshwater (1 g L^{-1} NaCl) as high-salinity stream.

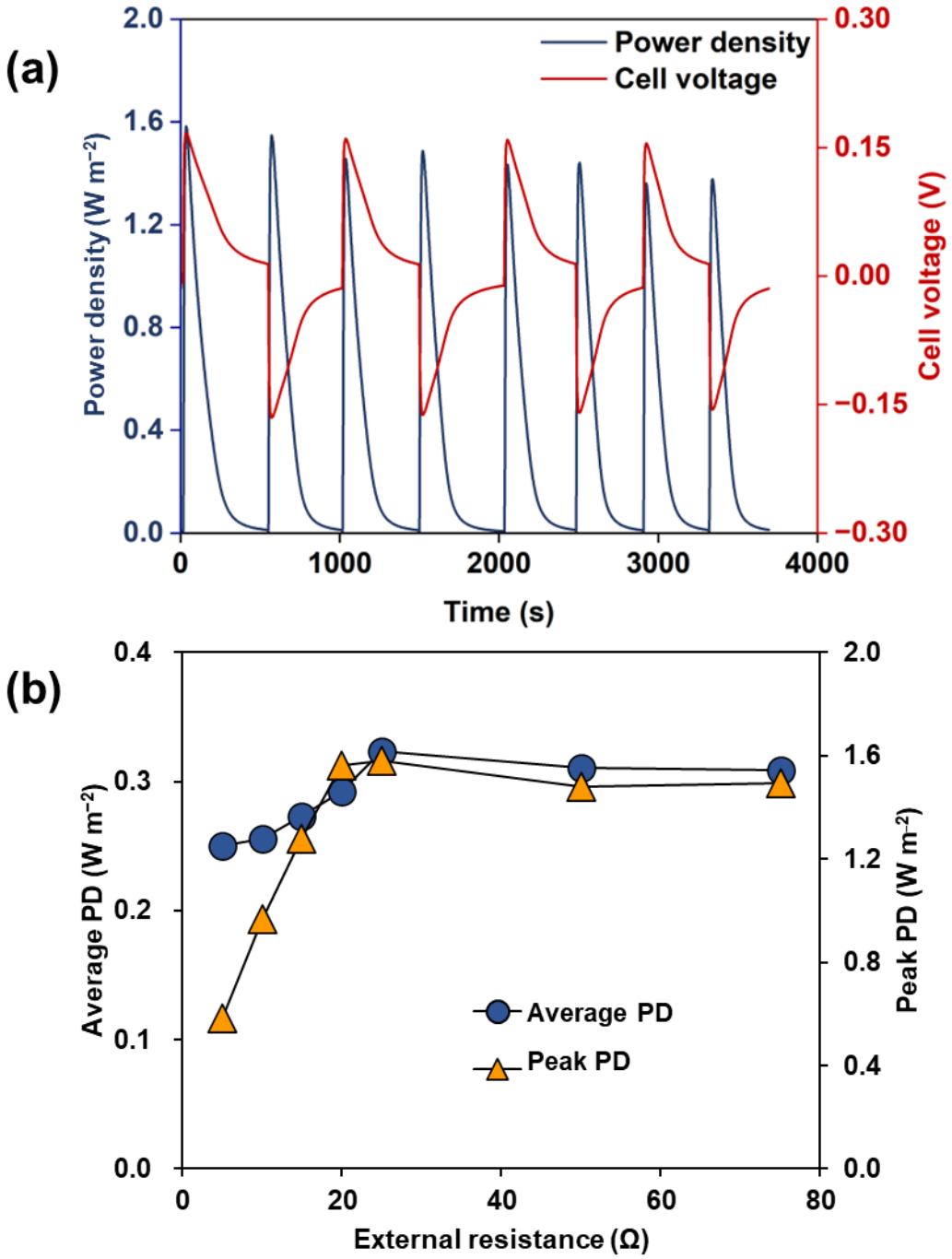

Fig. S5 Power generation performance of urine-ammonium power cell equipped with CuHCF electrodes, operated using 560 mM NH_4Cl solution (pH 4.9) and freshwater (1 g L^{-1} NaCl) as high- and low-salinity streams, respectively: (a) power density (PD) and cell voltage profiles at an external resistance of 25 Ω and (b) average and peak PD profiles as a function of external resistance.

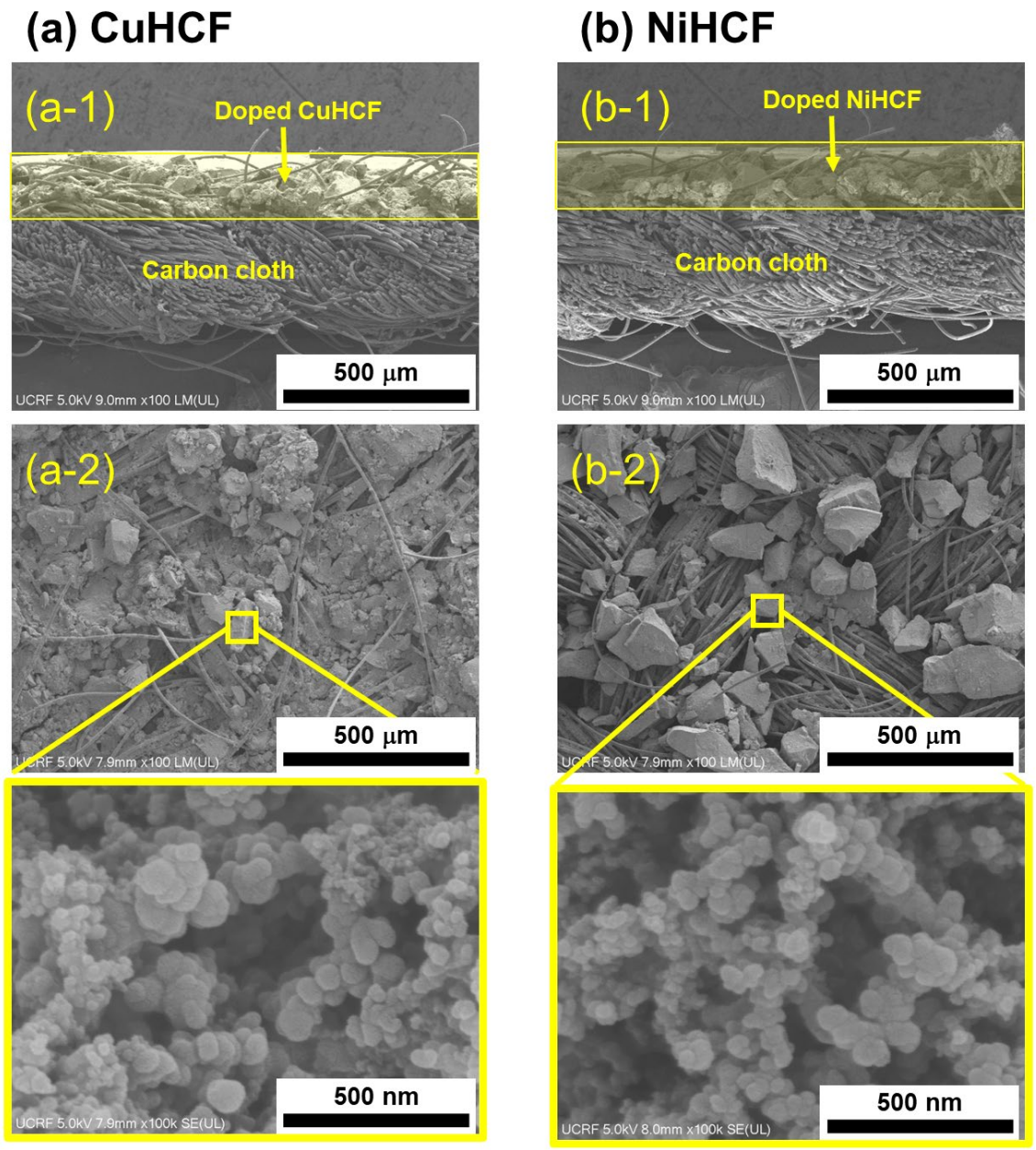

Fig. S6 Scanning electron microscopic images of (a) CuHCF and (b) NiHCF electrodes: (a-1, b-1) cross-sectional views and (a-2, b-2) surface views.

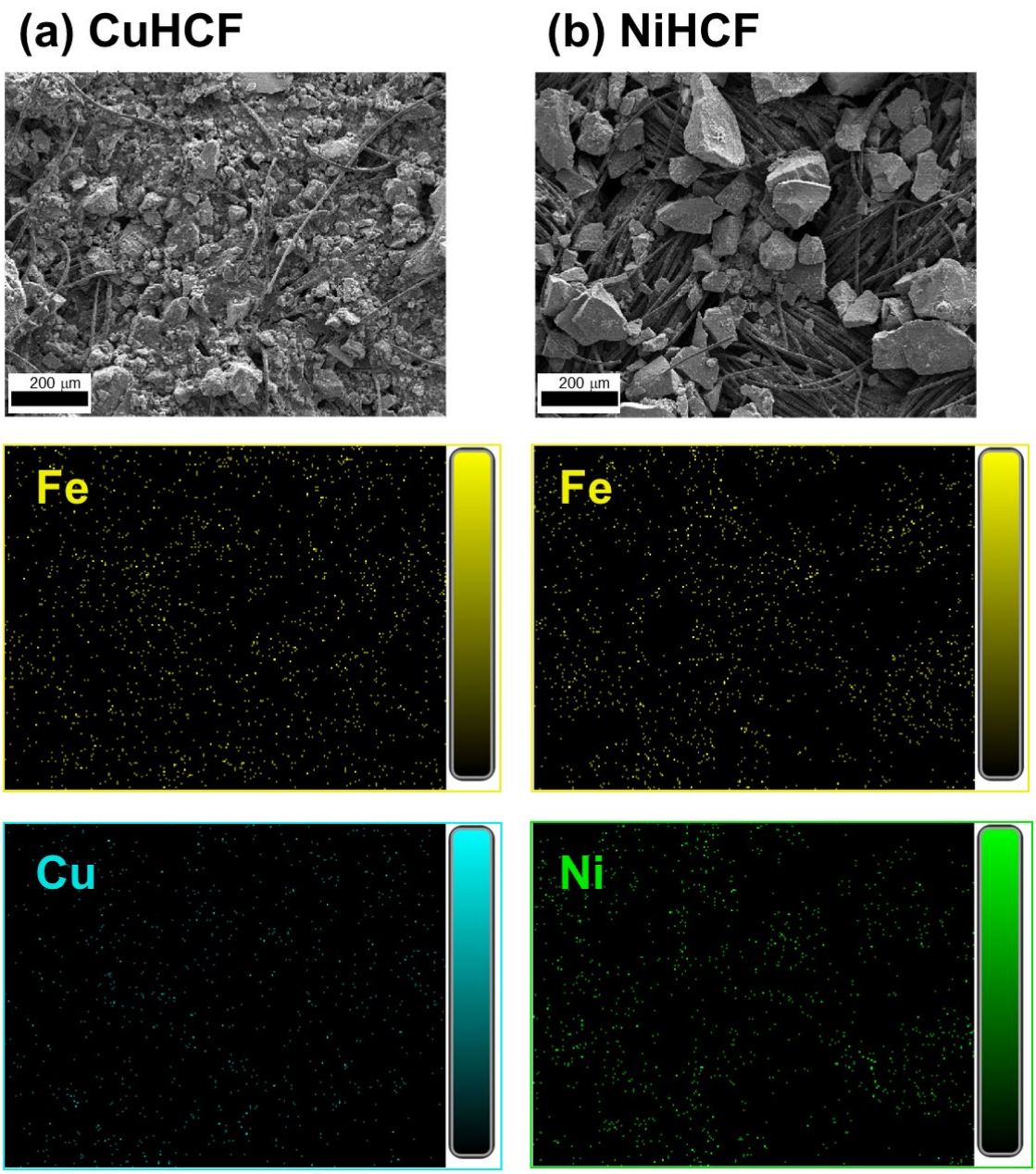

Fig. S7 Surface elemental distributions of (a) CuHCF and (b) NiHCF electrodes characterized by energy-dispersive X-ray spectroscopy.

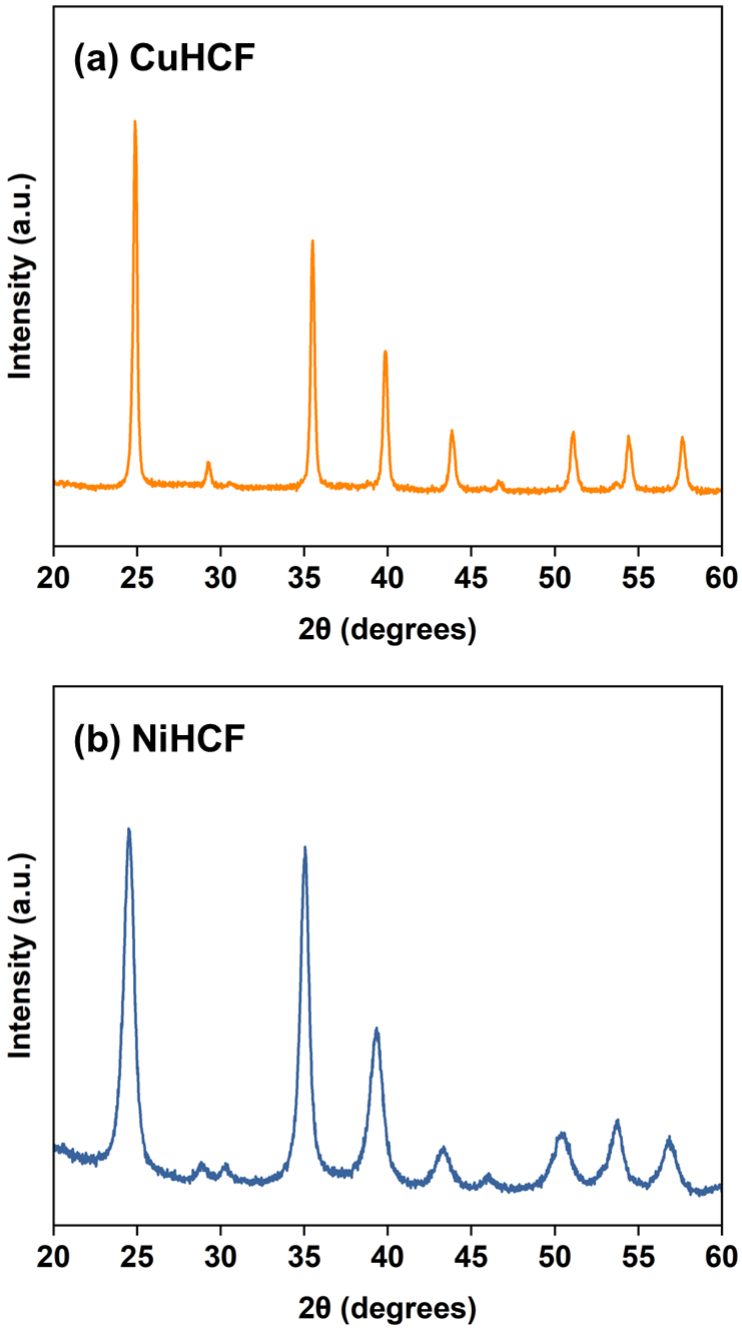

Fig. S8 X-ray diffraction patterns of synthesized (a) CuHCF and (b) NiHCF powders, confirming their crystalline characteristics.

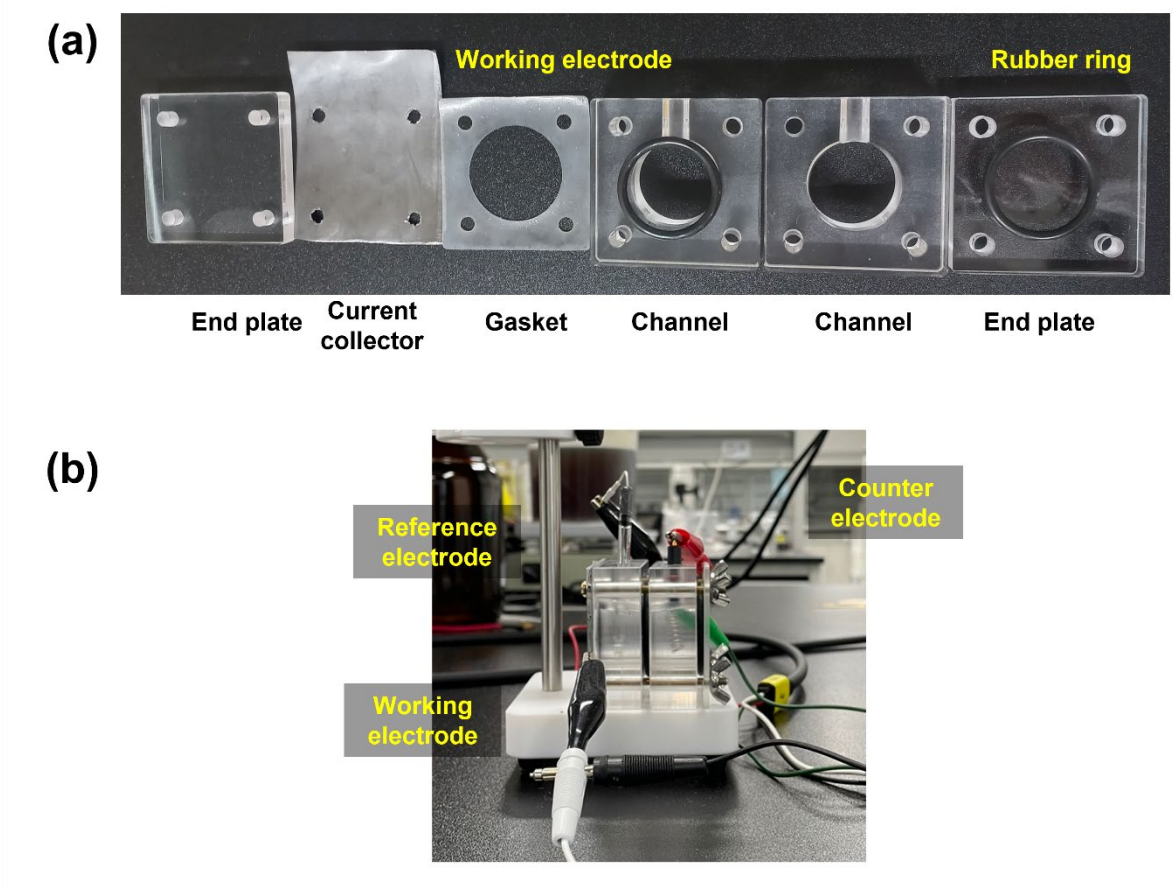

Fig. S9 Configuration of cyclic voltammetry cell: (a) photograph of disassembled components and (b) photograph of assembled three-electrode setup.